

## Supplementary information:

### S1. Microfabrication

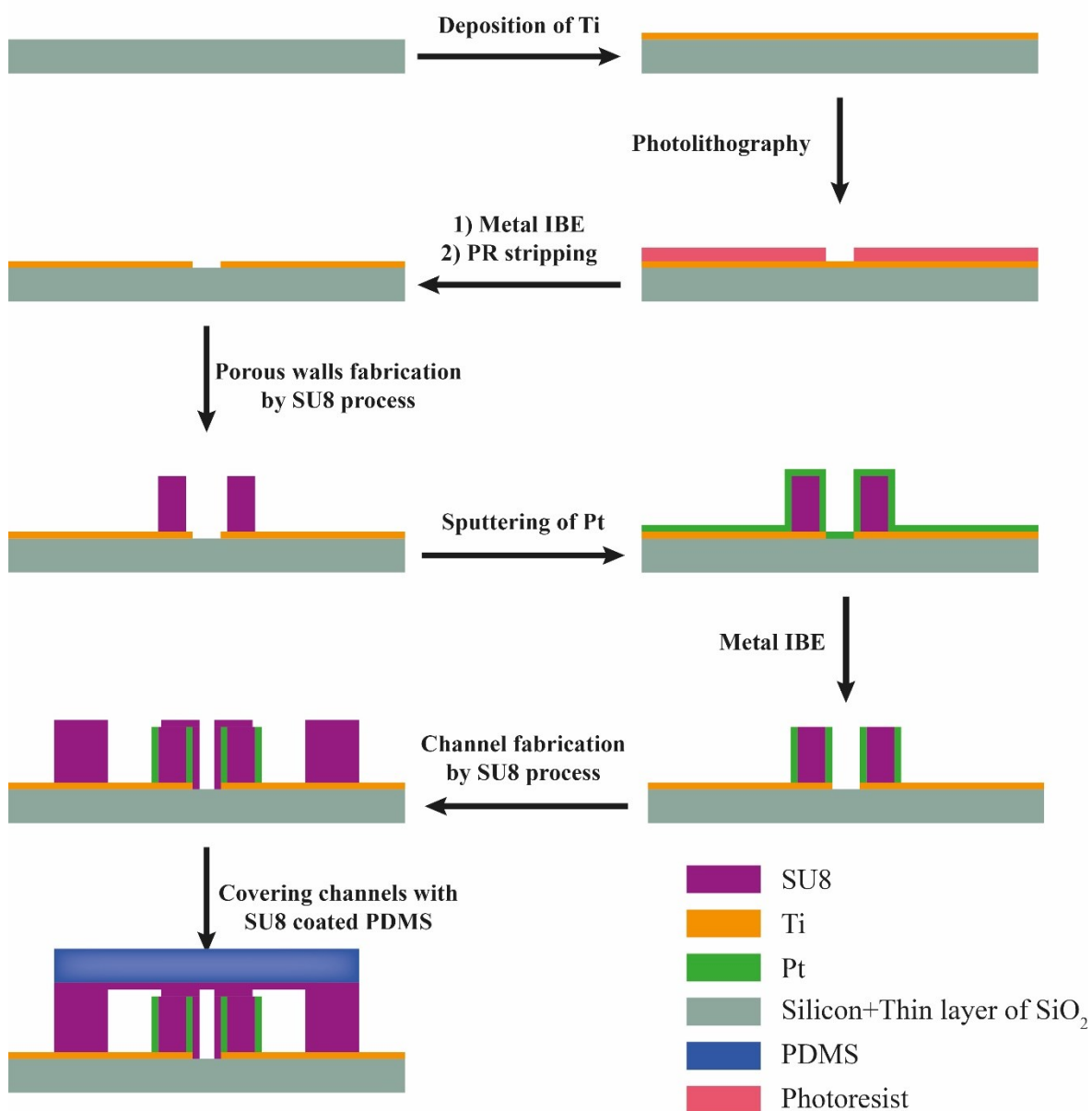


Figure S1. Fabrication process of the porous walls electrolyzer

## S2. Two phase pressure drop

The pressure drop of the multiphase flow is calculated by assuming the two-phase flow of gas and liquid. The gas phase is assumed to be a mixture of hydrogen and oxygen. Consequently, average density and viscosity of the mixture gas phase are used for the pressure drop calculation. These average properties are calculated by the following equations:

$$\bar{\rho}_G = y_{H_2}\rho_{H_2} + y_{O_2}\rho_{O_2} \quad (1)$$

and

$$\bar{\mu}_G = y_{H_2}\mu_{H_2} + y_{O_2}\mu_{O_2} \quad (2)$$

where  $y_i$  is the mole fraction of gas  $i$ ,  $\rho$  is the density, and  $\mu$  is the viscosity.  $\bar{\rho}_G$  and  $\bar{\mu}_G$  are the average density and viscosity of the gas mixture. The mole fraction of hydrogen and oxygen in the water electrolysis reaction are  $2/3$  and  $1/3$ , respectively.

The flow quality ( $x$ ) and the gas volume fraction ( $\alpha$ ) are needed to calculate the pressure drop. The flow quality is can be expressed as below:

$$x = \frac{M_{H_2} + M_{O_2}}{M_{total}} \quad (3)$$

where  $M_{H_2}$  and  $M_{O_2}$  are the mass flow rate of hydrogen and oxygen, respectively.  $M_{total}$  is the total mass flow rate of the electrolyte and gas. The mass flow rate of gas products are calculated using Faraday's electrochemical laws. The volume fraction of the mixture gas is defined as [1]:

$$\alpha = \frac{\rho_L x}{\bar{\rho}_G(1-x) + \rho_L x} \quad (4)$$

In equation (4),  $\rho_L$  is the electrolyte density. This equation assumes homogenous flow and unity gas/liquid velocity ratio.

The accelerational pressure drop is given by:

$$\Delta P_{acceleration} = \frac{M_{total}}{A} \left\{ \left[ \frac{(1-x)^2}{\rho_L(1-\alpha)} + \frac{x^2}{\rho_G\alpha} \right]_{out} - \left[ \frac{1}{\rho_L} \right]_{in} \right\} \quad (5)$$

where  $A$  is the cross sectional area. Subscripts in and out determine the inlet and outlet of the channel. Bubbles are being generated after the inlet. Therefore, the volume fraction of the gas phase is zero at the inlet.

The frictional pressure drop is calculated by the following equation [1]:

$$\Delta P_{friction} = \int_0^L \frac{32 M_{total}^2}{Re A \rho_{mixture}} dz \quad (6)$$

where  $L$ ,  $\rho_{mixture}$ , and  $Re$  are the length of the channel, two-phase mixture density, and Reynolds number.  $z$  is the direction of the flow. The  $Re$  is calculated by the following equation:

$$Re = \frac{\rho_{mixture} V D}{\mu_{mixture}} \quad (7)$$

In equation (7),  $\mu_{mixture}$  is the viscosity of the two-phase mixture.  $\rho_{mixture}$  and  $\mu_{mixture}$  are given by:

$$\frac{1}{\rho_{mixture}} = \frac{1-x}{\rho_L} + \frac{x}{\rho_G} \quad (8)$$

and

$$\frac{1}{\mu_{mixture}} = \frac{1-x}{\mu_L} + \frac{x}{\mu_G} \quad (9)$$

### S3. Effect of wall pores angle and size

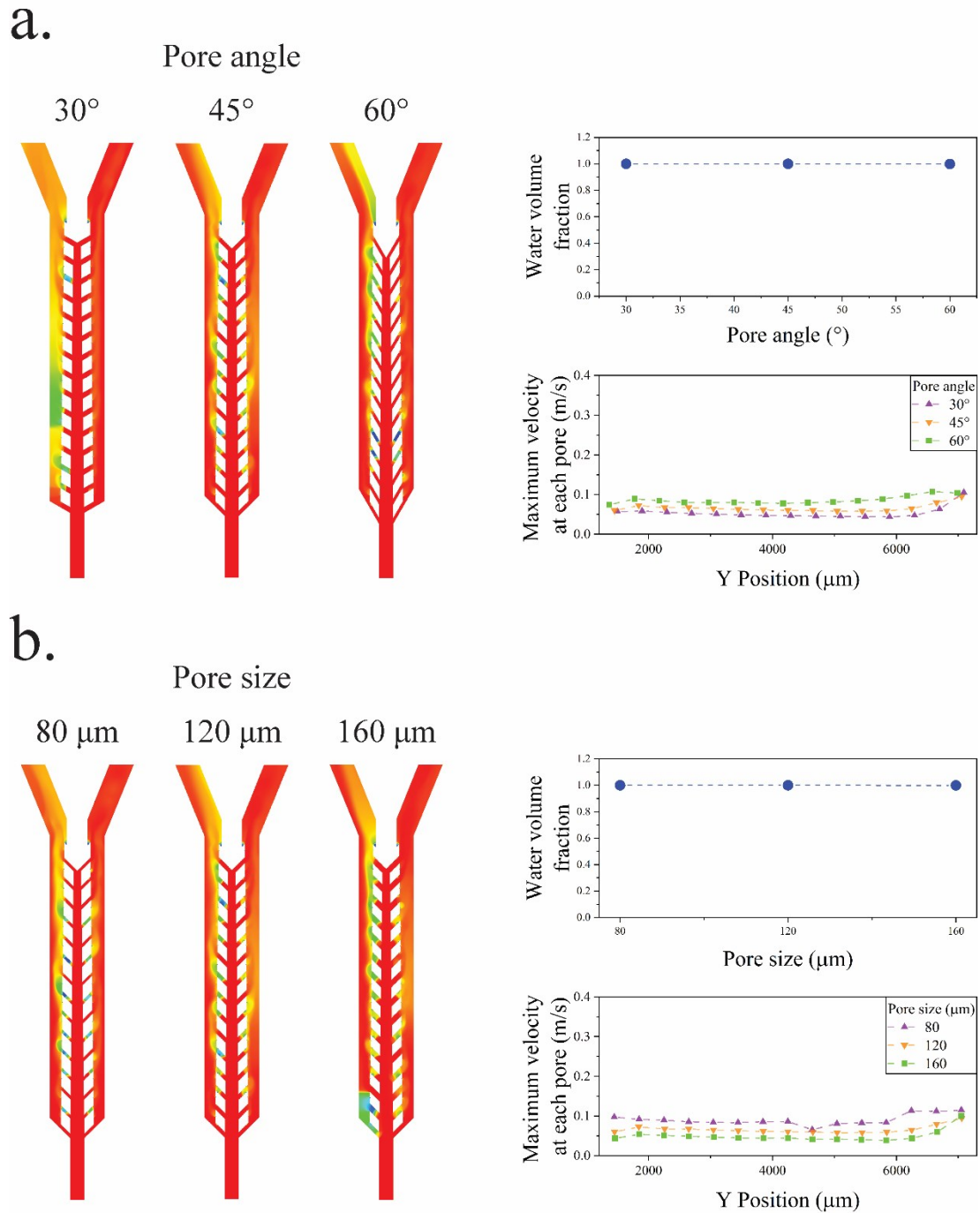
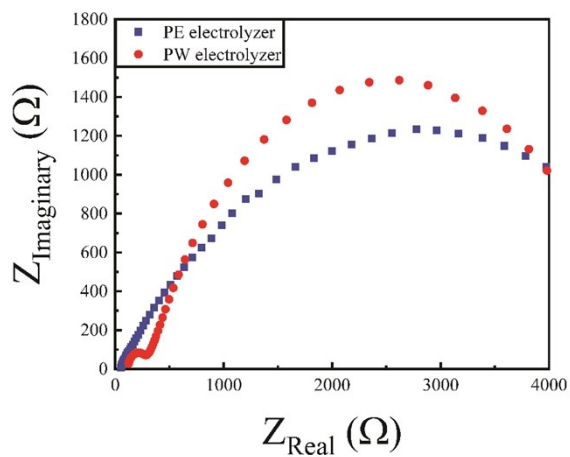


Figure S2. a. Changing the wall pores angle from 30° to 60° does not affect the velocity distribution in the pores or the water volume fraction in the middle channel. b. The velocity distribution in the pores remains uniform across the pores and the water volume fraction in the middle channel does not decrease when the pore size increases from 80 μm to 160 μm.

## S4. Potentio Electrochemical Impedance Spectroscopy (PEIS)

a.



b.

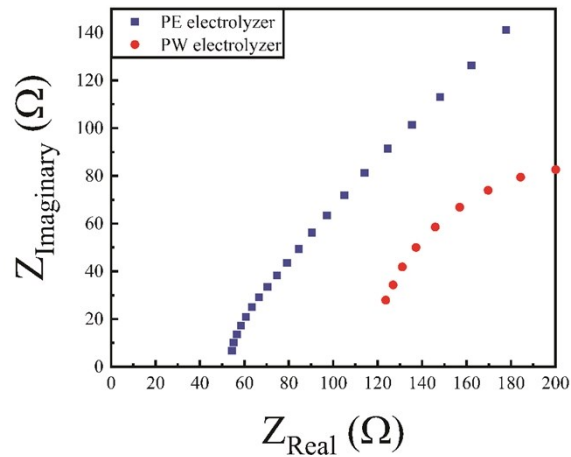


Figure S3. a. PEIS measurement of the PE and PW electrolyzers b. a magnified view of the PEIS measurement below  $200 \Omega$ . The electrolyte is 1 M sulfuric acid with  $10^{-4}$  M PFOS. The electrolyte flow rate is 80 ml/h. In this measurement, the applied potential and the sinus amplitude are 2.0 V and 20 mV, respectively.

## S5. Membrane-less electrolyzers

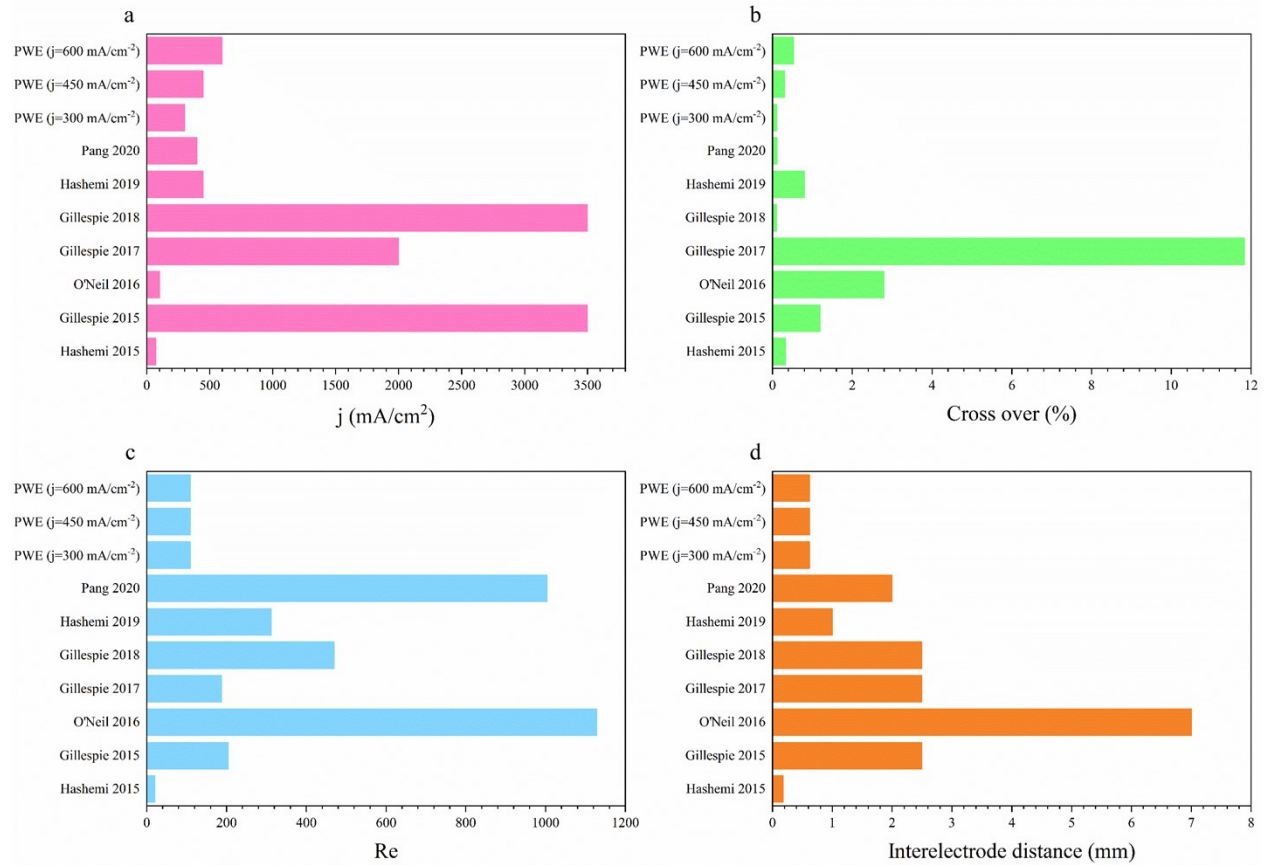


Figure S4. The current density (a), cross over (b), Re (c), and interelectrode distance (d) of membrane-less electrolyzers shown in Figure 9.

Some parameters in Figure S4 are calculated based on the data from the corresponding references. The data and calculated parameters for each reference are presented below:

The current density of the parallel electrodes electrolyzer of Hashemi et al. (2015) [2] is  $71.5 \text{ mA/cm}^2$  with a  $0.175 \text{ mm}$  interelectrode distance. The liquid flow rate and the channel cross-sectional area are  $14 \text{ ml/h}$  and  $61 \times 275 \mu\text{m}^2$ , respectively. The hydraulic diameter of the channel cross-section is used to calculate the Re. The electrolyte is  $1 \text{ M}$  sulfuric acid which its density and viscosity are  $1060 \text{ kg/m}^3$  and  $0.001208 \text{ Pa}\cdot\text{s}$  [3]. The cross over is extracted from Figure 5a of [2]. The current density and Re of the parallel electrodes membrane-less electrolyzer reported by Hashemi et al. (2019) [3] are  $450 \text{ mA/cm}^2$  and  $312$ , respectively. The cross over of this electrolyzer is extracted from Figure 6 of [3].

Gillespie et al. (2015) [4] reported a mesh electrodes electrolyzer working with  $30\%$  KOH electrolyte at  $3500 \text{ mA/cm}^2$ . The interelectrode distance of this device is  $3.5 \text{ mm}$ . The average cross-sectional velocity is  $0.075 \text{ m/s}$  across the electrode surface that has a  $30 \text{ mm}$  diameter. This velocity is used to calculate the velocity of the liquid at the periphery of the meshes which is  $0.45$

m/s. The density and viscosity of the 30 % KOH solution at room temperature are  $1288 \text{ kg/m}^3$  and  $0.0023 \text{ Pa}\cdot\text{s}$ , respectively [5-7]. The hydraulic diameter of the peripheral area is used to calculate the Re. The crossover of hydrogen to the oxygen side is calculated by using the reported hydrogen and oxygen purities assuming that the impurity in the oxygen side is hydrogen. The Re of Gillespie et al. (2017) [8] and Gillespie et al. (2018) [9] is calculated with similar procedures. The temperature of the electrolyte is  $80^\circ$  in [9] and [8]. At this temperature, the density and viscosity of the 30 % KOH solution are  $1260 \text{ kg/m}^3$  and  $0.001 \text{ Pa}\cdot\text{s}$ , respectively [5-7].

The membrane-less electrolyzer of O'Neil et al. (2016) [10] works at the current density of  $100 \text{ mA/cm}^2$  with 2.8 % hydrogen cross over to the oxygen side. The liquid velocity is  $0.265 \text{ m/s}$  and the channel area is  $13 \times 5 \text{ mm}^2$ . The liquid electrolyte is 0.5 M sulfuric acid with density =  $1030 \text{ kg/m}^3$  and viscosity =  $0.001102 \text{ Pa}\cdot\text{s}$ . The Re is calculated by considering the hydraulic diameter of the channel cross-section. The parallel electrodes electrolyzer of Pang et al. (2020) [11] has current density =  $400 \text{ mA/cm}^2$ , cross over = 0.12 %, and  $\text{Re} = 1004$ .

The working potential of these membrane-less electrolyzers is compared in Figure S5 at current density =  $300 \text{ mA/cm}^2$ . The potentials are extracted from the polarization curves.

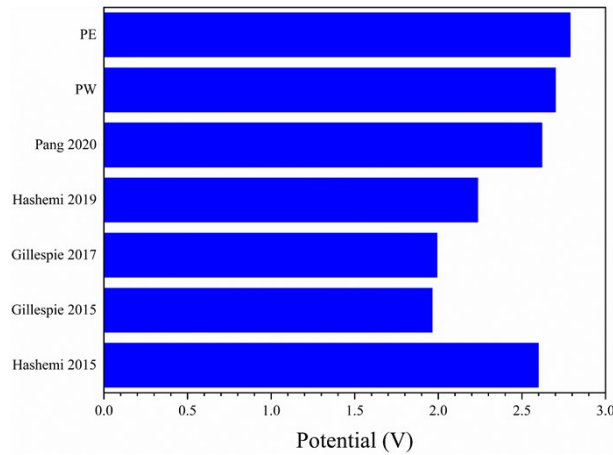


Figure S5. The working potential of membrane-less electrolyzers at current density =  $300 \text{ mA/cm}^2$ .

## References

1. Yadigaroglu, George and Geoffrey F Hewitt, *Introduction to multiphase flow: basic concepts, applications and modelling*. 2017: Springer.
2. Hashemi, S Mohammad H, Miguel A Modestino, and Demetri Psaltis, *A membrane-less electrolyzer for hydrogen production across the pH scale*. *Energy & Environmental Science*, 2015. **8**(7): p. 2003-2009.
3. Hashemi, S Mohammad H, Petr Karnakov, Pooria Hadikhani, Enrico Chinello, Sergey Litvinov, Christophe Moser, Petros Koumoutsakos, and Demetri Psaltis, *A versatile and membrane-less electrochemical reactor for the electrolysis of water and brine*. *Energy & Environmental Science*, 2019. **12**(5): p. 1592-1604.
4. Gillespie, MI, F Van Der Merwe, and RJ Kriek, *Performance evaluation of a membraneless divergent electrode-flow-through (DEFT) alkaline electrolyser based on optimisation of electrolytic flow and electrode gap*. *Journal of Power Sources*, 2015. **293**: p. 228-235.
5. Le Bideau, Damien, Philippe Mandin, Mohamed Benbouzid, Myeongsub Kim, and Mathieu Sellier, *Review of necessary thermophysical properties and their sensitivities with temperature and electrolyte mass fractions for alkaline water electrolysis multiphysics modelling*. *International Journal of Hydrogen Energy*, 2019. **44**(10): p. 4553-4569.
6. Sipos, Pal M, Glenn Hefter, and Peter M May, *Viscosities and densities of highly concentrated aqueous MOH solutions ( $M^{+} = Na^{+}, K^{+}, Li^{+}, Cs^{+}, (CH_3)_4N^{+}$ ) at 25.0° C*. *Journal of Chemical & Engineering Data*, 2000. **45**(4): p. 613-617.
7. Akerlof, Gosta and Paul Bender, *The density of aqueous solutions of potassium hydroxide*. *Journal of the American Chemical Society*, 1941. **63**(4): p. 1085-1088.
8. Gillespie, MI and RJ Kriek, *Hydrogen production from a rectangular horizontal filter press Divergent Electrode-Flow-Through (DEFT™) alkaline electrolysis stack*. *Journal of Power Sources*, 2017. **372**: p. 252-259.
9. Gillespie, MI and RJ Kriek, *Scalable hydrogen production from a mono-circular filter press Divergent Electrode-Flow-Through alkaline electrolysis stack*. *Journal of Power Sources*, 2018. **397**: p. 204-213.
10. O'Neil, Glen D, Corey D Christian, David E Brown, and Daniel V Esposito, *Hydrogen production with a simple and scalable membraneless electrolyzer*. *Journal of The Electrochemical Society*, 2016. **163**(11): p. F3012.
11. Pang, Xueqi, Jonathan T Davis, Albert D Harvey III, and Daniel V Esposito, *Framework for evaluating the performance limits of membraneless electrolyzers*. *Energy & Environmental Science*, 2020.